

# Nanomodified Fillers in Chloroprene-Rubber-Compatibilized Natural Rubber/Acrylonitrile–Butadiene Rubber Blends

Shaji P. Thomas,<sup>1</sup> E. J. Mathew,<sup>2</sup> C. V. Marykutty<sup>3</sup>

<sup>1</sup>Postgraduate Department of Chemistry, B. A. M. College, Thuruthicad, Affiliated with M. G. University, Kottayam, Kerala, India

<sup>2</sup>Research Department of Chemistry, S. B. College, Changanasserry, Affiliated with M. G. University, Kottayam, Kerala, India

<sup>3</sup>Department of Chemistry, Assumption College, Changanasserry, Affiliated with M. G. University, Kottayam, Kerala, India

Received 18 April 2011; accepted 2 August 2011

DOI 10.1002/app.35406

Published online 29 November 2011 in Wiley Online Library (wileyonlinelibrary.com).

**ABSTRACT:** Because of the structural dissimilarity, natural rubber (NR) and acrylonitrile–butadiene rubber (NBR) are immiscible, and compatibilizers are used during their blending. Neoprene or chloroprene rubber (CR) has a polar chlorine part and a nonpolar hydrocarbon part. Also, it has many advantageous properties, such as oil resistance, toughness, a dynamic flex life, and adhesion capacity. Hence, it is not less scientific to use CR as a compatibilizer in the blending of NBR with NR. Because many fewer studies on the use of neoprene as a compatibilizer in NR–NBR blend preparation are available, efforts were made to prepare 20:80 NR–NBR blends with CR with the aim of studying the effect of poly(ethylene oxide) (PEO)-coated nano calcium silicate along with nano *N*-benzylimine aminothioformamide and stearic acid coated nano zinc oxide in the sulfur vulcanization of the blends. The optimum dosage of

the compatibilizer was derived by the determination of the tensile properties, tear resistance, abrasion resistance, compressions set, and swelling values. The tensile strength, tear resistance, and abrasion resistance of the gum vulcanizates of the blend were improved by the compatibilizing action of CR up to 5 parts per hundred parts of rubber (phr). In the case of the filled vulcanizates, the tear resistance, 300% modulus, hardness, and abrasion resistance increased with increasing dosage of nano calcium silicate. The elongation at break percentage decreased as expected when there was an increase in the modulus. Scanning electron microscopy was used to study the phase morphology of the blends. © 2011 Wiley Periodicals, Inc. *J Appl Polym Sci* 124: 4259–4267, 2012

**Key words:** blends; mechanical properties; nanoparticle; vulcanization

## INTRODUCTION

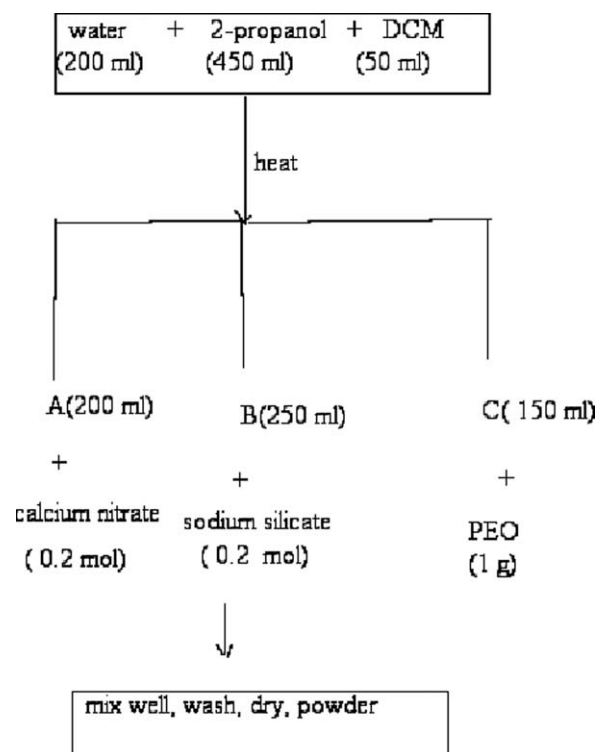
A considerable amount of research has been done over the last several years with a view to obtaining new polymeric materials with enhanced specific attributes for specific applications. Much attention has been devoted to the simplest route for combining the outstanding properties of different existing polymers, that is, by blending polymers. Although increasing numbers of miscible blends have been reported,<sup>1–5</sup> most polymers are, nonetheless, immiscible; this leads to heterophase polymer blends. There are two widely useful types of elastomeric blends: miscible single-phase and immiscible two-phase blends.

It is well established that the presence of certain polymeric species with the right structure can indeed result in the compatibilization of an immiscible elastomer blend because of their ability to alter the interfacial situation.<sup>6–8</sup> Such species, known as *compatibilizers*, are added or formed *in situ* during the blending of elastomers. The compatibilizers in elastomer blends have manifold roles, such as (1) reducing the interfacial energy between the phases, (2) permitting a finer dispersion during mixing, (3) providing a measure of stability against gross segregation, and (4) resulting in improved interfacial adhesion.<sup>9,10</sup> Two elastomers form a compatible blend when they satisfy any one of the following characteristics: they have (1) segmental structural identity or (2) miscibility/partial miscibility with each other [the difference in the solubility parameter ( $\delta$ ) should desirably be less than 0.2 units] or (3) functional groups capable of generating covalent or other bonds between the polymers.<sup>6,11</sup>

Compatibilization of dissimilar elastomer blends is an area of active interest from both the technological and scientific points of view. Many synthetic and

Correspondence to: E. J. Mathew (mathewetolil@rediffmail.com).

Contract grant sponsor: University Grants Commission of India.



**Scheme 1** Synthesis of nano-PEO-coated calcium silicate.

natural elastomers have good properties that when combined with other similar or complementary properties, may yield desirable traits in the products. Kader et al.<sup>12</sup> prepared a 50/50 natural rubber (NR)/acrylonitrile-butadiene rubber (NBR) blend using *trans*-polyoctylene rubber as a compatibilizer. They showed that the inclusion of *trans*-polyoctylene rubber in the blend altered the phase morphology by reducing the size of the NBR phase. Sirisinha et al.<sup>13</sup> proved that the oil resistance of a 20/80 NR-NBR blend depended strongly on the phase morphology of the blend. The smaller the size of the NR dispersed phase was, the higher was the resistance to oil. Mathai et al.<sup>14</sup> concluded that the equilibrium solvent uptake decreased with an increase in the concentration of NBR.

Chloroprene rubber (CR) has a backbone structure similar to that of NR but is more polar because of a chlorine substituent. The solubility parameter value of CR is intermediate to that of NR and NBR. Also, the presence of a dipole within the repeat unit allows the possibility of the interaction of the acrylonitrile repeat unit of NBR. Kantala et al.<sup>15</sup> investigated the effect of fly ash particles on the vulcanizate properties of NR-NBR blends compatibilized by CR. Kala<sup>16</sup> also investigated the thermal properties and surface morphology of NR-NBR blends.

Unlike NR, NBR has appreciable resistance to hydrocarbon oil. NR is easily available in our state, and hence, the blending of NBR with NR is carried out to reduce the cost of products that require inher-

ent NBR properties.<sup>17,18</sup> Because only very few studies have been reported on CR-compatibilized NR-NBR blends, especially those containing surface-modified nanofillers, we attempted to investigate the effects of PEO-coated nano calcium silicate along with nano *N*-benzylimine aminothioformamide (nano-BIAT) and zinc oxide (ZOS) on the curing and mechanical properties of CR-compatibilized 20/80 NR-NBR blends.<sup>13-18</sup> The nanomodified fillers were characterized by Fourier transform infrared (FTIR) spectroscopy and scanning electron microscopy (SEM) studies. The vulcanizate properties, such as the tensile properties, tear resistance, abrasion resistance, compressions set, and swelling values, were investigated. The phase morphology was studied by SEM.

## EXPERIMENTAL

### Rubber and ingredients

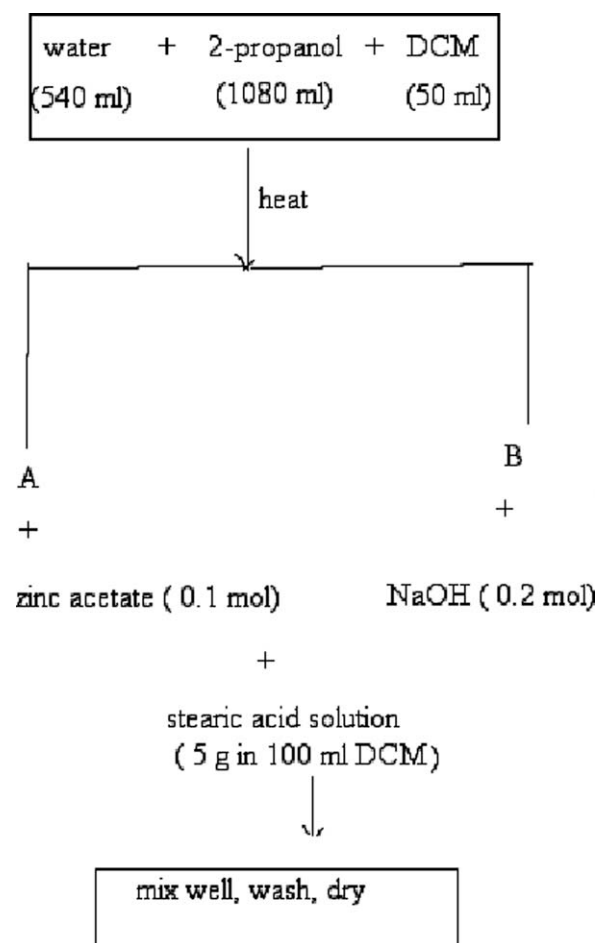
NBR (33% acrylonitrile content, grade N-684) was supplied by Eliokom Pvt., Ltd. (Gujrat, India), and NR (grade ISNR-5) was supplied by RRII (Kottayam, India). Rubber-grade stearic acid, *N*-cyclohexyl benzothiazyl sulfenamide (CBS), diethylene glycol (DEG), naphthenic oil, and sulfur were supplied by Ceynar Rubber Chemicals (Kottayam, India). We prepared the nanomodified filler, PEO-coated calcium silicate, per Scheme 1.<sup>19,20</sup> The synthesis and characterization of nano-BIAT and nano-ZOS are given in Schemes 2 and 3, respectively.<sup>21,22</sup>

### Synthesis of the nano-PEO-coated calcium silicate

Water (200 mL), 2-propanol (450 mL), and dichloromethane (DCM; 50 mL) were mixed and heated to 60°C. The hot solution was divided into three portions. Calcium nitrate (0.2 mol) was dissolved in 200 mL of the ternary solution, 0.2 mol of sodium silicate was dissolved in 250 mL of the ternary solution, and 1 g of PEO was dissolved in the remaining solution. With continuous stirring, the sodium silicate solution was added to the calcium nitrate solution; this was followed by the addition of the PEO solution. After it was stirred for another 10 min, the mixture was allowed to stand for 5 h and was then filtered, washed, and dried in a vacuum oven at 60–70°C. The white solid was powdered in a ball mill (Laxmi Engineers, Jodhpur, India).

### Preparation of the NR-NBR blend

NR (20 phr) was masticated for 2 min, and CR was added to it and homogenized by many passes in a two-roll mixing mill (15.3 × 30.5 cm<sup>2</sup>, Indian Expeller, Ahmedabad, India) at a friction ratio 1 : 1.14 as per ASTM D 3182-89. NBR (80 phr) was also masticated separately as done previously and then added to the

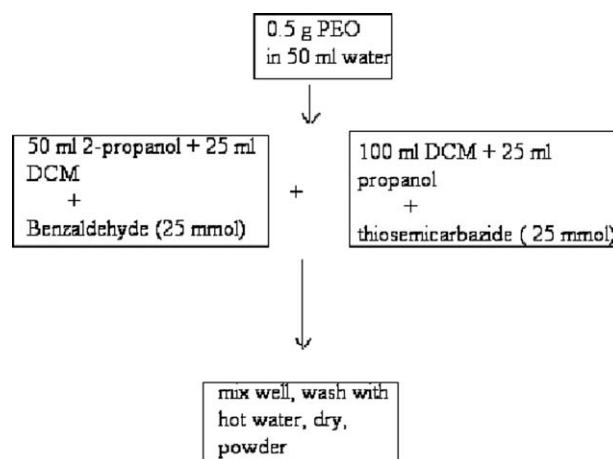


Scheme 2 Synthesis of ZOS.

NR-CR mixture. The mastication was continued for 5–7 min until a homogeneous blend was obtained.

#### Unfilled blend formulations

NB<sub>1</sub>–NB<sub>5</sub> (Table I) represent the 20/80 NR–NBR blend unfilled formulations. These were prepared by



Scheme 3 Synthesis of nano-BIAT.

thorough mixing of the 20/80 NR–NBR blend obtained as discussed previously with 5 phr nano-ZOS, the binary accelerator system of 1.32 phr CBS, 1.3425 phr nano-BIAT, and 1.5 phr sulfur (S) in the order indicated in Table I. Amounts of 2, 3, 4, 5, and 6 phr CR, respectively, were placed in the NB<sub>1</sub>–NB<sub>5</sub> mixes. CR was not added to NB<sub>R</sub> during blending.

#### Filled blend formulations

NBF<sub>1</sub>–NBF<sub>4</sub> represent the 20/80 NR–NBR blend filled formulations compatibilized by 5 phr CR (Table I). NBF<sub>1</sub> contained 5 phr nano calcium silicate, 1 phr naphthenic oil, and 1 phr DEG in addition to other ingredients, as in the case of the unfilled formulations. NBF<sub>2</sub> contained 10 phr nano calcium silicate, NBF<sub>3</sub> contained 15 phr nano calcium silicate, and NBF<sub>4</sub> contained 20 phr nano calcium silicate. NBF<sub>5</sub> contained 7 phr nano calcium silicate plus 3 phr Cloisite 93A clay, and NBF<sub>6</sub> contained 7 phr nanoclay alone. The dosages of ZOS, CBS, nano-BIAT, S, DEG, and oil remained the same with the

TABLE I  
NBR–NBR Blend Formulations Containing Nano Calcium Silicate

Ingredient	Mix											
	NB <sub>1</sub>	NB <sub>2</sub>	NB <sub>3</sub>	NB <sub>4</sub>	NB <sub>5</sub>	NB <sub>R</sub>	NBF <sub>1</sub>	NBF <sub>2</sub>	NBF <sub>3</sub>	NBF <sub>4</sub>	NBF <sub>5</sub>	NBF <sub>6</sub>
NR	20	20	20	20	20	20	20	20	20	20	20	20
NBR	80	80	80	80	80	80	80	80	80	80	80	80
CR	2	3	4	5	6	0	5	5	5	5	5	5
ZOS	5	5	5	5	5	0	5	5	5	5	5	0
ZnO	0	0	0	0	0	5	0	0	0	0	0	5
Stearic acid	0	0	0	0	0	2	0	0	0	0	0	2
CBS	1.32	1.32	1.32	1.32	1.32	1.32	1.32	1.32	1.32	1.32	1.32	1.32
Nano-BIAT	1.3425	1.3425	1.3425	1.3425	1.3425	0	1.3425	1.3425	1.3425	1.3425	1.3425	1.3425
Micro-BIAT	0	0	0	0	0	1.3425	0	0	0	0	0	0
Nano calcium silicate	0	0	0	0	0	0	5	10	15	20	7	0
Cloisite 93A	0	0	0	0	0	0	0	0	0	0	3	7
DEG	0	0	0	0	0	0	1	1	1	1	1	0
Naphthenic oil	0	0	0	0	0	0	1	1	1	1	1	1
S	1.5	1.5	1.5	1.5	1.5	1.5	1.5	1.5	1.5	1.5	1.5	1.5

**TABLE II**  
Cure Properties of the NBR–NBR Mixes Containing Nano Calcium Silicate

Mix	$t_{90}$	$t_{s2}$	Minimum torque (dNm)	Maximum torque (dNm)	CRI
NB1	5.9	1.2	0.5	5.4	21.28
NB2	4.8	1.3	0.6	5.6	28.57
NB3	3.7	1.3	0.7	5.8	41.67
NB4	3.8	1.2	0.5	5.8	38.46
NB5	6.2	1.3	0.4	5.2	20.41
NBR	6.3	1.3	0.4	5.2	18.37
NBF1	5.1	1.2	0.2	4.2	25.64
NBF2	4.6	1.5	0.2	5.1	32.26
NBF3	3.2	1.3	0.4	5.5	52.63
NBF4	3.7	1.4	0.3	4.6	43.48
NBF5	4.5	1.1	0.4	5.2	29.41
NBF6	4.6	1.2	0.5	5.2	29.41

exception that no DEG was taken in NBF<sub>6</sub>. The mixes were prepared in the same two-roll mill after we followed the same procedure described previously.

### Evaluation of the curing properties

The optimum cure time ( $t_{90}$ ) of the mixes (the time to reach 90% of the maximum torque) was determined on a Goettfert elastograph (Vario model, 74722 Buchen, Germany) at 150°C. The cure properties were obtained directly, and the values are given in Table II. The elastographic scorch time ( $t_{s2}$ ) is the time required for two units to increase above the minimum torque (ca. 10% vulcanization). The compounds were then vulcanized up to the optimum cure time in an electrically heated laboratory-type hydraulic press (Indian Expeller) at 150°C at a pressure of 120 kg/cm<sup>2</sup> to obtain sheets for the determination of the tensile and tear properties, circular buttons for abrasion loss, and compression set determination.

### Tensile properties and tear resistance

The tensile properties of the vulcanized samples were determined on a universal testing machine (series IX model 4411, Instron Corp., Grove City, Pennsylvania) at a crosshead speed of 500 mm/min as per ASTM D 412-87 with dumbbell-shaped specimens.

### Hardness

Hardness (Shore A) was measured as per ASTM D 2240-86 with a Zwick 3114 (Zwick USA, 1620 Cobb International Blvd., Kennesaw) hardness tester on unstressed, molded cylindrical samples (diameter = 30 mm, thickness = 6 mm). For each vulcanized sample, three measurements were taken, and the result reported is the average.

### Compression set

The compression set was determined as per ASTM D 395-89 (method B) with an apparatus manufac-

tured by Prolific Engineers India, Ltd., (Noida, India). The molded samples (1.25 cm thick and 2.8 cm in diameter) in duplicate and compressed to a constant deflection (25%) were kept for 22 h at 27°C. The samples were taken out, and after 30 min, the final thickness was measured. The compression set was calculated by Eq. (1):

$$\text{Compression set(\%)} = \frac{(t_0 - t_1) \times 100}{t_0 - t_s} \quad (1)$$

where  $t_0$  and  $t_1$  are the initial and final thicknesses of the specimen and  $t_s$  is the thickness of the space bar used. For each molded sample, the average of the duplicate measurements is reported as the final result.

### Abrasion loss

The abrasion loss was measured with a DIN abrader (DIN 53516, Prolific Engineers India Ltd, Noida, India). A molded sample having a diameter of  $6 \pm 0.2$  mm and a thickness of 6 mm was inserted into the sample holder so that 2 mm of the sample remained exposed and was allowed to move across the surface of an abrasive sheet mounted on a revolving drum. The weights of the test specimen were noted before and after the test. The difference in weight was converted into volume loss by division of the weight loss by the density of the specimen. Three molded samples of each mix were used for the determination of abrasion loss, and the final result is expressed as the average of these results.

### Swelling value

Circular samples approximately 1 cm in diameter, 0.2 cm thick, and with a weight of 0.2 g were punched out from the central portions of the vulcanizate and allowed to swell in toluene for 24 h. The swollen samples were taken out and weighed again after we removed the solvent on the surface of the samples using blotting paper. The solvent was removed *in vacuo*, and the weight of the deswollen sample was again noted to calculate the swelling value ( $Q$ )<sup>23</sup> for each sample as an indicator of the crosslink density<sup>24</sup> of the vulcanizates with Eq. (2):

$$Q = \frac{(W_s - W_d) \times W_R}{100W_1} \quad (2)$$

where  $W_s$  is the weight of the solvent-swollen samples,  $W_d$  is the weight of the deswollen samples,  $W_1$  is the weight of the preswollen samples, and  $W_R$  is the weight of the recipe (total weight of all of the components in the mix, including rubber).



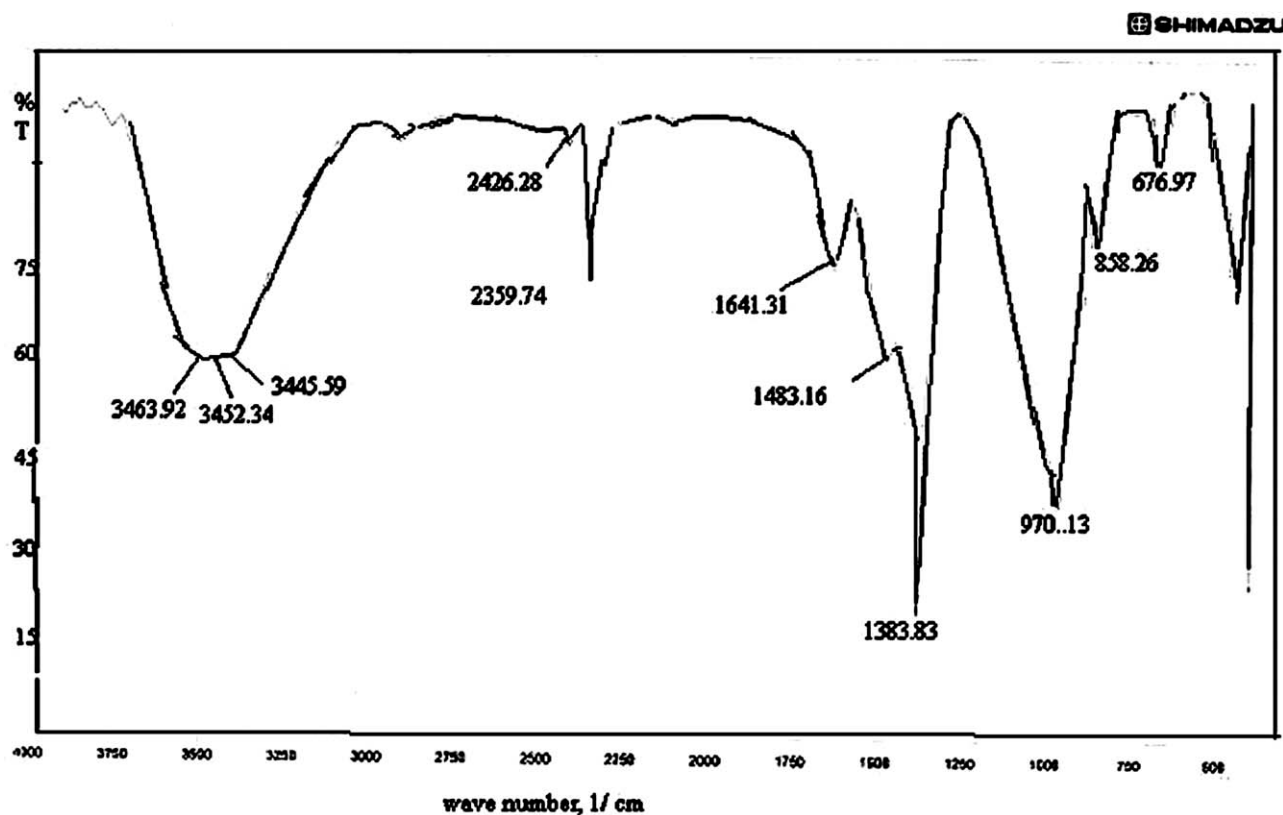


Figure 1 FTIR spectrum of nano calcium silicate.

## RESULTS AND DISCUSSION

### Characterization of the nanofillers

Sodium silicate reacted with calcium nitrate in the ternary solution to form calcium silicate. The PEO particles could act as nuclei for the development of calcium silicate nanoparticles. In addition to this, because of the presence of polar oxygen and the nonpolar hydrocarbon part of the PEO molecules, they could reduce the surface energy of the calcium particles and, thereby, reduce the particle-particle interaction. Thus, the agglomeration of silicate particles was reduced; this was similar to the effect of stearic acid in nano-ZnO production. The nanoparticles of calcium silicate produced by this sol-gel precipitation were characterized by FTIR spectroscopy (Fig. 1) and SEM imaging [Fig. 3(a), shown later]. The band  $970\text{ cm}^{-1}$  was due to Si-O stretching, and that at  $676.97\text{ cm}^{-1}$  was due to Si-O-Si bending vibrations.<sup>25</sup> The particles were almost globular and below 50 nm in dimension. The band at  $858.26\text{ cm}^{-1}$  was due to the rocking vibrations of  $(\text{CH}_2)_n$  of PEO, the bands at 1483 and  $1383\text{ cm}^{-1}$  were due to asymmetric  $(\text{CH}_2)_n$  bending and symmetric  $(\text{CH}_2)_n$  wagging, respectively, and the band at  $1641\text{ cm}^{-1}$  was due to the C-O stretching of PEO.<sup>26</sup>

### Curing properties of the unfilled NR-NBR blends

The  $t_{90}$  values exhibited a decrease from NB<sub>1</sub>, which contained 2 phr CR, to NB<sub>3</sub>, which contained 4 phr CR (Table II). There was no considerable decrease for the NB<sub>4</sub> mix, which contained 5 phr CR. The decrease in  $t_{90}$  could have been due to better NR-NBR interaction made possible by the enhanced compatibilization as the dosage of CR increased. Beyond 5 phr CR, a further increase could not contribute to compatibilization; instead, the excess dosage of CR required additional time for curing. Because CR contained polar segments containing chlorine, it could establish new interaction with the polar acrylonitrile segment of NBR, and at the same time, the hydrocarbon segment of CR got attached to NR and, thus, acted as a binding agent, as shown in Figure 2. The presence of CR, thus, could have increased the finer dispersion and improved the interfacial adhesion between the component polymer chains. All of the mixes showed almost the same scorch safety ( $t_{s2}$ ) values, and this indicated that minor CR contents did not affect the scorch safety. The torque change value (Maximum torque - Minimum torque), which was directly related to the extent of crosslinking,<sup>27,28</sup> increased with dosage of CR up to 5 phr and then showed a decrease because the optimum compatibilization and, hence, the maximum miscibility of the NR and NBR

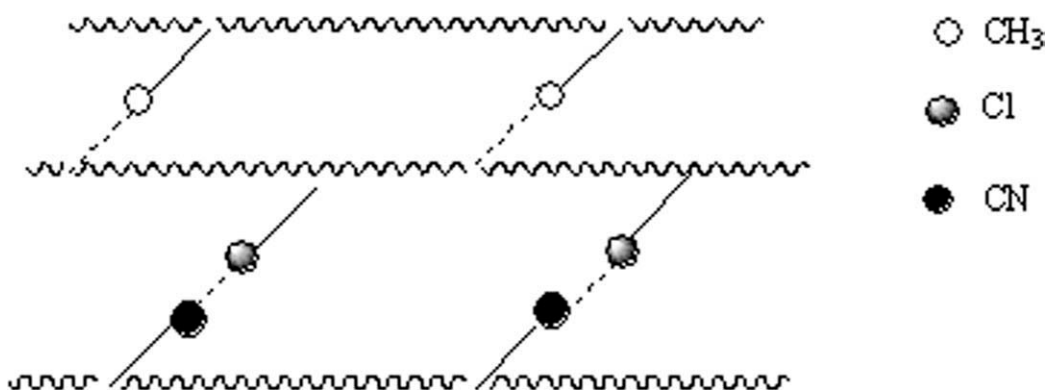
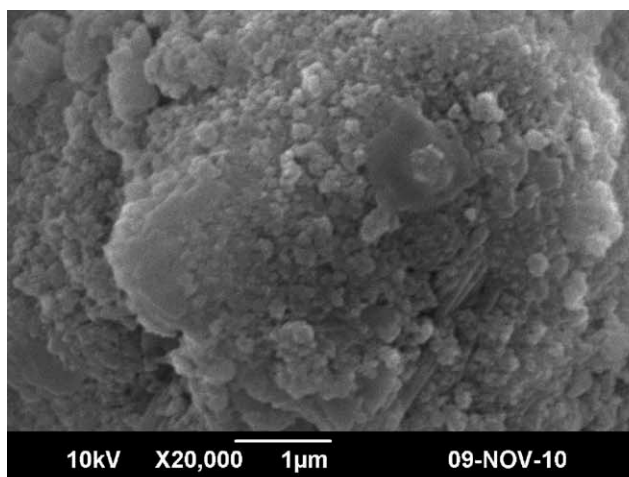


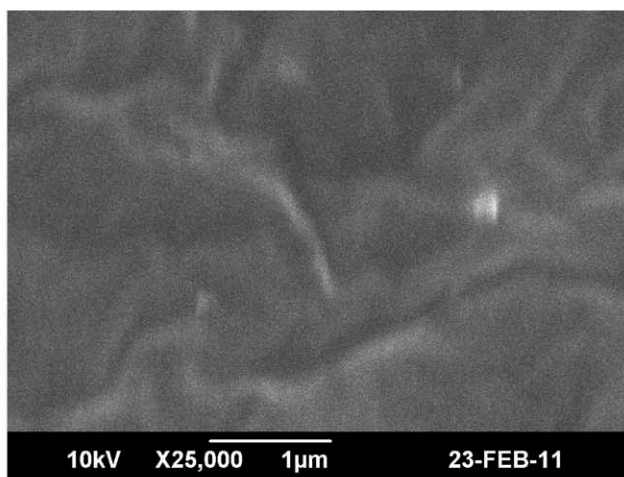
**Figure 2** Schematic representation of the compatibilizing action of CR in the NR-NBR blend

phases occurred at 5 phr CR (mix NB<sub>4</sub>). The cure rate index (CRI), calculated as  $100/(t_{90} - t_{s2})$ , also exhibited an increase with the dosage of CR and was minimum for 6 phr CR (NB<sub>5</sub>), which showed better curing for the NR-NBR (20/80) blend compatibilized by 5

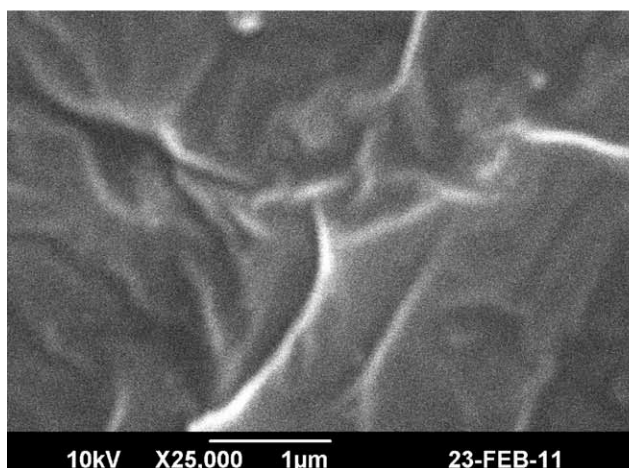
phr CR because of the better dispersion of NR in NBR, as evident from the SEM images [Fig. 3(b,c)]. The wide bandlike structures in the SEM image of NB<sub>R</sub> indicated high phase separation, which was less pronounced in NB<sub>4</sub>.



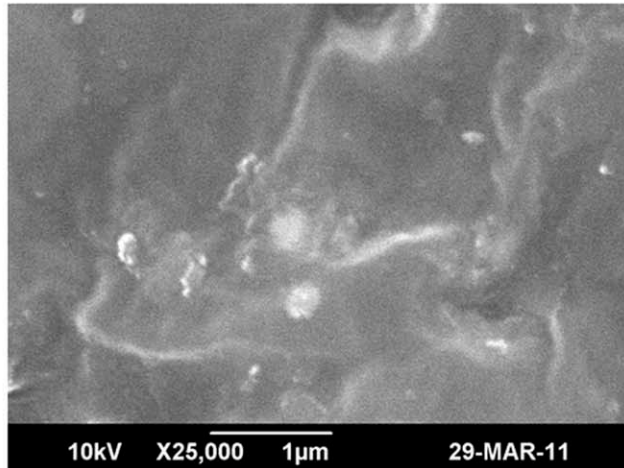
(a)



(b)



(c)



(d)

**Figure 3** SEM images of (a) nano calcium silicate, (b) NB<sub>4</sub>, (c) NB<sub>R</sub>, and (d) NBF<sub>2</sub>.

**TABLE III**  
**Physicomechanical Properties of NBR-NBR Mixes Containing Nano Calcium Silicate**

Mixes	Tensile strength (MPa)	300% modulus (MPa)	Elongation at break (%)	Tear resistance (N/mm)	Compression set (%)	Shore A hardness	Abrasion loss (cm <sup>3</sup> )	Swelling value
NB <sub>1</sub>	3.79 ± 0.060	2.11 ± 0.0015	379 ± 4	14.97 ± 0.060	4.2	36 ± 0.6	0.186 ± 0.0004	2.95
NB <sub>2</sub>	4.51 ± 0.070	2.09 ± 0.0010	398 ± 2	18.63 ± 0.055	4.39	36 ± 0.6	0.185 ± 0.0004	2.91
NB <sub>3</sub>	5.13 ± 0.076	2.08 ± 0.0015	419 ± 4	20.95 ± 0.079	4.43	37 ± 0.6	0.182 ± 0.0004	2.88
NB <sub>4</sub>	6.81 ± 0.061	2.01 ± 0.0006	463 ± 4	21.63 ± 0.057	4.62	38 ± 0.6	0.171 ± 0.0004	2.81
NB <sub>5</sub>	4.11 ± 0.066	2.32 ± 0.0015	378 ± 4	18.61 ± 0.056	4.53	38 ± 0.6	0.185 ± 0.0005	2.93
NB <sub>R</sub>	3.65 ± 0.087	2.19 ± 0.0015	362 ± 4	13.69 ± 0.090	4.18	38 ± 0.6	0.187 ± 0.0005	2.97
NBF <sub>1</sub>	5.94 ± 0.085	2.09 ± 0.0012	436 ± 5	17.92 ± 0.060	3.89	39 ± 0.6	0.181 ± 0.0008	2.85
NBF <sub>2</sub>	5.72 ± 0.085	2.11 ± 0.0015	422 ± 5	18.78 ± 0.096	3.56	40 ± 0.6	0.174 ± 0.0006	2.89
NBF <sub>3</sub>	4.92 ± 0.050	2.32 ± 0.0015	398 ± 6	19.98 ± 0.076	3.12	40 ± 0.6	0.168 ± 0.0006	2.92
NBF <sub>4</sub>	4.61 ± 0.080	2.41 ± 0.0012	374 ± 6	22.12 ± 0.056	2.81	40 ± 0.6	0.163 ± 0.0007	2.95
NBF <sub>5</sub>	4.28 ± 0.076	2.69 ± 0.0012	337 ± 6	23.63 ± 0.060	3.05	40 ± 0.6	0.169 ± 0.0006	2.99
NBF <sub>6</sub>	4.8 ± 0.085	2.32 ± 0.0012	398 ± 6	20.81 ± 0.085	3.21	39 ± 0.6	0.171 ± 0.0006	2.97

### Tensile properties

The tensile strength increased with increasing dosage of CR up to 5 phr (mix NB<sub>4</sub>) and then decreased (Table III) as in the case of the torque change value. The sulfidic crosslinking between the component polymer chains and the NR-CR-NBR chains increased with the dosage of CR up to the optimum concentration of CR in the mix NB<sub>4</sub>. The presence of CR increased the finer dispersion and improved the interfacial adhesion<sup>10</sup> between the component polymer chains; this increased the miscibility and homogenization of the NR and NBR mixture, as was clear from SEM [Fig. 3(b)]. As the miscibility of NR in the NBR phase increased, an improvement in the tensile strength was expected. Beyond the optimum dosage of CR, the extra phase formed by CR caused a minor reduction in the tensile strength of the blend. The 300% modulus values showed a minor reduction up to 5 phr CR (mix NB<sub>4</sub>), which could have been due to the increase in the miscibility of NR in the NBR phase. As the NR miscibility increased, the elasticity increased, and hence, the stiffness decreased.<sup>29</sup> However, beyond 5 phr CR, no more CR was required to increase the miscibility of NR in the NBR phase, and hence, the excess CR remaining in the blend caused an increase in the stiffness of the blend vulcanizate, which could have resulted in the slight increase in the modulus value of the mix NB<sub>5</sub>.

The elongation at break percentage values exhibited an increase from NB<sub>1</sub> to NB<sub>4</sub>; this was in agreement with the decrease in the 300% modulus values. The mix NB<sub>5</sub> had a lower elongation at break percentage because of the presence of more CR than that required for the maximum homogenization of NR and NBR.

The mix NB<sub>R</sub>, which contained rubber-grade ZnO, stearic acid, and micro-BIAT as a binary accelerator showed inferior curing and tensile properties; this

indicated that the dispersion of the activator, coactivator, and accelerator was at a maximum and homogeneous for nanomodified forms (ZOS and nano-BIAT), as we proved in our earlier studies.

### Tear resistance

The tear resistance increased from NB<sub>1</sub> to NB<sub>4</sub> as the dosage of CR increased from 2 to 5 phr; this showed that NR miscibility in the NBR phase increased, and hence, the dispersion and homogenization of phases were at maxima at 5 phr CR (Table III). The mix NB<sub>5</sub> showed a slight reduction in the tear resistance value because of the presence of a greater quantity of CR than that required for the optimum compatibilization of the NR and NBR phases. Thus, crosslinking increased from NB<sub>1</sub> to NB<sub>5</sub>.

### Hardness and compression set (%)

All of the mixes had almost comparable hardness values, with a slight increase as the dosage of CR increased. The increased CR content increased the hardness of the NB<sub>3</sub>-NB<sub>5</sub> mixes.

Compressions set percentage values of all of the mixes up to NB<sub>3</sub> were almost comparable, although a slight increase was noted. This could have been due to the reduction in the modulus of the vulcanizates. Because the excess dosage of CR imparted a higher stiffness to the mix NB<sub>5</sub>, it exhibited a slightly lower compression set percentage.

### Abrasion loss

Although the mixes exhibited comparable abrasion loss, the mix NB<sub>4</sub> had minimum abrasion loss (maximum abrasion resistance). This could also have been due to maximum crosslinking in the highest compatibilized blend.



### Swelling values

The swelling values of the vulcanizates were in agreement with the mechanical properties investigated. A decreasing trend was observed from NBR up to NB<sub>4</sub>; this indicated the maximum crosslink density for it.

### Nanofilled formulations

#### Cure properties

The cure time decreased as the dosage of nano calcium silicate increased from 5 to 15 phr (NBF<sub>1</sub>–NBF<sub>3</sub>; Table II). All of the mixes showed comparable scorch safety ( $t_{s2}$ ) values. The torque change values increased slightly with increasing dosage of nano calcium silicate; this indicated a better curing state. CRI showed an increasing trend from NBF<sub>1</sub> to NBF<sub>3</sub>; this indicated a better dispersion of nano calcium silicate, as proven for nanoparticles such as nano-CaCO<sub>3</sub>, nanoclay, and carbon nanotubes in different elastomer matrices with a two-roll mill.<sup>30,31</sup> A slight increase in the curing time was observed for NBF<sub>4</sub> and could have been due to the presence of an excess of silicate.

However, the presence of clay in NBF<sub>5</sub> and NBF<sub>6</sub> caused a reduction in CRI. The mix NBF<sub>6</sub>, which contained 7 phr nanoclay, exhibited a similar cure time as the mix NBF<sub>2</sub>, which contained 10 phr silicate; this indicated that the nano calcium silicate synthesized in our laboratory and nanoclay purchased were almost equally dispersed in the polymer matrix. The mix NBF<sub>5</sub>, which contained 7 phr calcium silicate and 3 phr nanoclay also exhibited curing properties comparable with those of the NBF<sub>6</sub> mix.

#### Tensile properties

As the dosage of nano calcium silicate was increased from 5 to 15 phr, the tensile strength decreased slightly (Table III). This could have been due to the migration of curatives<sup>32</sup> (adsorbed on to the surface of nanosilicate particles) to the more polar NBR, which caused poor vulcanization of NR in the presence of silicate particles. The percentage elongation at break values were in agreement with this observation. Among the mixes containing silicate only (NBF<sub>1</sub>–NBF<sub>4</sub>), NBF<sub>4</sub> exhibited a minimum percentage elongation at break value because of the higher modulus. As the concentration of nanosilicate increased, the elongation at break decreased. The SEM image of NBF<sub>2</sub> [Fig. 2(d)] showed that nano calcium silicate particles were as uniformly dispersed in the polymer matrix as the nanoclay particles in NBF<sub>6</sub>. Only very few agglomerates were seen in the SEM image of NBF<sub>2</sub>. The presence of 3

phr nanoclay along with 7 phr nano calcium silicate caused a reduction in tensile strength of NBF<sub>5</sub> when compared with NBF<sub>1</sub>, NBF<sub>2</sub>, and NBF<sub>3</sub>. This could have been due to a failure of synergism<sup>13</sup> between the calcium silicate and clay, which had a similar chemical nature. The presence of clay reduced the elongation at break and increased the modulus of the vulcanizate NBF<sub>5</sub>. However, the mix NBF<sub>6</sub>, which contained 7 phr nanoclay, exhibited a higher tensile strength and percentage elongation at break than the mixes NBF<sub>4</sub> and NBF<sub>5</sub> because of the better dispersion of the lower quantity of nanoclay present in the mix (in NBF<sub>4</sub> and NBF<sub>5</sub>, higher dosages of filler were present; this could have led to agglomeration).

#### Tear resistance

As the dosage of nano calcium silicate increased from 5 to 20 phr, the tear resistance also increased; this could have been due to the increase in the surface area of the filler<sup>25</sup> and the increased rubber–filler interaction (Table III). As the filler surface increased, it could more effectively hinder the crack propagation. The presence of 3 phr nanoclay along with 7 phr nano calcium silicate in NBF<sub>5</sub> increased the tear resistance because of the additive action of the individual components. The tear resistance of the mix containing 15 phr nano calcium silicate (NBF<sub>3</sub>) and that containing 7 phr nanoclay (NBF<sub>6</sub>) alone were almost comparable; this showed in the elastomer matrix efficiency of nano calcium silicate for its better dispersion as the nanoclay.

#### Abrasion loss

As the dosage of nano calcium silicate increased from 5 to 15 phr, the abrasion loss decreased (and the abrasion resistance increased) because of the increase in the filler–rubber interaction.<sup>25</sup> The uniform dispersion of nano calcium silicate increased the filler–rubber interaction, and maximum abrasion resistance was, thus, observed for NBF<sub>4</sub>. The mixes containing nanoclay alone or in combination with other fillers (NBF<sub>6</sub> and NBF<sub>5</sub>) exhibited a slightly higher abrasion loss, as expected for clay.

#### Compression set (percentage)

As the dosage of calcium silicate increased, the compression set percentage decreased. This could have been due to the increase in stiffness. The value was found to be minimum for NBF<sub>5</sub> because of its maximum stiffness. The mix NBF<sub>6</sub> had a comparable set to that of the mix NBF<sub>3</sub> in accordance with its modulus.



### Hardness (Shore A)

As the dosage of the silicate filler increased, the hardness also increased. The clay-filled mix NBF<sub>6</sub> showed a slight reduction in the hardness, which could have been due to the lower dosage of clay and its specific nature.

### Swelling values

The swelling values, which are a measure of cross-link density, of the vulcanizates were in agreement with the mechanical properties investigated. The lower swelling values indicated a high crosslink density. Among the silicate-filled vulcanizates, NBF<sub>1</sub> and NBF<sub>2</sub> exhibited minimum and comparable swelling values (Table III). This could have been due to the uniform dispersion of nanosilicate in the polymer matrix. At a lower concentration of nanosilicate, the agglomeration was minimum, and hence, the voids in the rubber lattices were occupied by the filler particles; this reduced the solvent intake.

## CONCLUSIONS

CR could function as a compatibilizer in the blending of NBR with NR. The gum vulcanizates of the CR-compatibilized NBR-NBR (80 : 20) blend possessed better tensile strength, tear resistance, abrasion resistance, and hardness compared to the uncompatibilized blend. Compatibilization reached a maximum for 5 phr CR. The investigations with nano calcium silicate alone and in combination with nanoclay showed that nano calcium silicate were as effective as nanoclay in imparting good tensile strength, tear resistance, compression set, hardness, and abrasion resistance to the NR-NBR blend. Better properties were obtained for the NR-NBR blend with 7 phr nano calcium silicate and 3 phr Cloisite 93 A clay, although a slight reduction in the tensile strength was observed. The better dispersion of nanoparticles in the CR-compatibilized NBR-NBR blend caused an improvement in the technological properties.

The authors thank Sabu Thomas (Director, School of Chemical Sciences, M. G. University, Kerala), Sumitra Sen Gupta (Rajeev Gandhi Centre for Biotechnology, Trivandrum), P. A. Najeeb (Director), and R. Arjunan Pillai (Technical Officer, Common Facility Service Centre, Verror, Kerala) for providing the instrument facilities.

## References

- Datta, S.; Lohse, D. J. *Polymeric Compatibilizers*; Hanser: New York, 1996.
- Polymer Blends and Alloys*; Shonaike, G. O., Simon, G. P., Eds.; Marcel Dekker: New York, 1999.
- Multi Component Polymer Systems*; Miles, I. S., Rostami, S., Eds.; Longman: London, 1992.
- Polymer Blends Handbook*; Utrachi, L. A., Ed.; Kluwer Academic: Dordrecht, The Netherlands, 2002; Vols. 1 and 2.
- Tinker, A. J. *Rubber Chem Technol* 1990, 63, 503.
- Arjunan, P. U.S. Pat. 5,352,739 (1994).
- Ismail, M. N.; El-Sabbagh, S. H.; Yehia, A. A. *J Elastomers Plast* 1999, 31, 3.
- Abdellah, A.; Utracki, L. A. *Polym Eng Sci* 1996, 36, 1574.
- Majumdar, B.; Keskkula, H.; Paul, D. R. *Polymer* 1994, 35, 3164.
- Molau, G. E. In *Block Copolymers*; Agarwal, S. L., Ed.; Plenum: New York, 1970; p 79.
- Tinker, A. J. In *Industrial Composites Based on Natural Rubber*; Malaysian Rubber and Development Board: Kuala Lumpur, 1998; p 103.
- Kader, M. A.; Kim, W. D.; Kaang, S.; Nah, C. *Polym Int* 2005, 54, 120.
- Sirisinha, C.; Limcharoen, S.; Thunyarittikom, J. *J Appl Polym Sci* 2003, 87, 83.
- Mathai, A. E.; Singh, R. P.; Thomas, S. J. *Membr Sci* 2002, 202, 35.
- Kantala, C.; Wimolmala, E.; Sirisinha, C.; Sombatsompop, N. *Polym Adv Technol* 2009, 20, 448.
- Kala, A. *IUP J Phys* 2009, 2, 7.
- Sirisinha, C.; Sae-Oui, P. *J Appl Polym Sci* 2003, 90, 4038.
- El-Sabbagh, S. H.; Yehia, A. A. *Egypt J Solids* 2007, 30, 157.
- Mishra, S.; Shimpi, N. G. *J Sci Ind Res* 2005, 64, 744.
- James, H. J.; Thomas, B.; Daniel, R.; Mathew, C.; James, E. G.; Andrew, M. *Curr Appl Phys* 2008, 8, 504.
- Nawaz, H. R.; Solangi, B. A.; Zehra, B.; Nadeem, U. *Canadian J Sci Ind Res* 2011, 2, 164.
- Thomas, S. P.; Ettolil, M. J. *J Appl Polym Sci* 2010, 121, 2257.
- Aprem, A. S.; Mathew, G.; Joseph, K.; Thomas, S. *Kautsch Gummi Kunstst* 1999, 52, 576.
- Flory, P. J.; Rehner, J. *J Chem Phys* 1943, 11, 521.
- Anik, M.; Laszl, R.; Herwig, P.; Janos, R.; Shiro, K.; Peter, H.; Katalin, S. J. *Phys Chem A* 2010, 114, 1040.
- Manorathel, C. H.; Rajapakse, R. M. G.; Dissanayake, M. A. K. L. *Int J Electrochem Sci* 2006, 1, 32.
- Arroyo, M.; Lopez-Manchado, M. A.; Herrero, B. *Polymer* 2003, 44, 2447.
- Wolff, S.; Wang, M. J.; Tan, E. H. *Rubber Chem Technol* 1993, 66, 163.
- Sirisinha, C.; Sae-Oui, P.; Guaysomboon, J. *J Appl Polym Sci* 2003, 87, 83.
- Leon, D. P.; Manuel, A. Z.; Thein, K.; James, E. M.; Betty, L. L. *Polym Eng Sci* 2009, 49, 866.
- Mishra, S.; Shimpi, N. G. *J Sci Ind Res* 2005, 64, 744.
- Das, A.; Ghosh, A. K.; Basu, D. K. *Kautschuk Gummi Kunstst* 2002, 84, 22.